Synthesis, Structural Characterization, and Metalation of *N*-*o*-Tolyl-5,10,15,20-tetraphenylporphine: Deformation Effect Due to a Bulky N-Substituent Group

Sen-ichi Aizawa,[1] Yasuyuki Tsuda,[2] Yoshio Ito,[2] Keiichiro Hatano,[3] and Shigenobu Funahashi*,[1]

Laboratory of Analytical Chemistry, Faculty of Science, Nagoya University, Chikusa, Nagoya 464-01, Faculty of Pharmacy, Meijo University, Tempaku, Nagoya 466, and Department of Pharmaceutical Sciences, Nagoya City University, Nagoya 467, Japan

Received June 2, 1992

The tetraphenylporphyrin with a bulky N-substituent group, *N*-*o*-tolyl-5,10,15,20-tetraphenylporphine (H(*o*-TolTPP)) has been synthesized and characterized by ^{1}H NMR spectroscopy, secondary ion mass spectrometry, UV–visible spectrophotometry, and an X-ray crystal structure analysis. The free base porphyrin (H(*o*-TolTPP)·$^1/_2C_6H_6$·$^1/_2NC_4H_{11}$) crystallizes in the triclinic space group $P\bar{1}$ with $Z = 2$ and lattice parameters $a = 9.054(1)$ Å, $b = 15.369(4)$ Å, $c = 16.963(3)$ Å, $\alpha = 70.30(1)°$, $\beta = 75.64(1)°$, $\gamma = 89.42(2)°$, $V = 2145(15)$ Å^3. The final R value is 0.092. The assignment and characterization of the ^{1}H NMR signals have been confirmed on the basis of its crystal structure. The N-substituted pyrrole ring is tilted from the N1–N2–N4 reference porphyrin plane by 57.3(2)° and three other pyrrole rings by −19.3(2)°, 1.6(10), and −16.4(2)°, respectively. The porphyrin ring system for H(*o*-TolTPP) is highly distorted from planarity in comparison with that for the N-methylated porphyrin. The kinetics for metalation of H(*o*-TolTPP) with zinc(II) ion revealed that the distortion of the porphine core is favorable to the complexation rate. The second-order rate constant at 25 °C and activation parameters are as follows: $k = 35 \pm 1$ mol^{-1} kg s^{-1}, $\Delta H^* = 39 \pm 2$ kJ mol^{-1}, and $\Delta S^* = -88 \pm 6$ J K^{-1} mol^{-1}. The kinetic properties are discussed in terms of steric effects.

Introduction

Stereochemical and kinetic studies of metalloporphyrins are important in order to understand the metal ion incorporation in vivo.[4-8] It is also possible to use porphyrins for microanalyses of metal ions because of their high extinction coefficients if metalloporphyrin formation can become more rapid.[9,10] In the extensive studies of N-substituted porphyrins especially by Lavallee et al.,[11-27] it has been found that *N*-alkylporphyrins form metal complexes much faster than the corresponding non-N-alkylated porphyrins.[23-25] Subsequently, we have studied the reaction mechanism of metalloporphyrin formation for *N*-methyl-5,10,15,20-tetraphenylporphine (H(MeTPP)) by a high-pressure stopped-flow technique.[28] In these studies, it has been suggested that the properties of *N*-alkylporphyrins different from non-N-alkylated porphyrins are attributed to the distortion from planarity of the aromatic ring system for the free-base porphyrins. On the other hand, only a few structures of neutral free-base N-substituted porphyrins have been reported[11] though the structures of a number of transition metal complexes of N-substituted porphyrins[12-21] and protonated nonmetallo N-substituted porphyrins have been described.[22] Hence, further studies of the stereochemistry of the free base porphyrins are necessary in order to understand the relationship between the structures and kinetic properties of N-substituted porphyrins.

In this paper, we report the preparation and structural characterization of *N*-*o*-tolyl-5,10,15,20-tetraphenylporphine (H(*o*-TolTPP)) which has a much bulkier N-substituent group than the previously reported H(MeTPP).[23-25,28] These studies make it possible to clarify the steric effects of the N-substituent groups. We have also investigated the incorporation reaction of zinc(II) ion into H(*o*-TolTPP) in *N*,*N*-dimethylformamide (DMF) in connection with the structure.

Experimental Section

Materials. Reagent grade DMF was dried over Molecular Sieves 4A and distilled twice under reduced pressure. Reagent grade zinc(II) nitrate hexahydrate and sodium nitrate were recrystallized from distilled water. The crystals of zinc(II) nitrate were dissolved in DMF, and the water in the solution was removed under reflux for 6 h in a modified Soxhlet extractor with Molecular Sieves 4A in the thimble.[29,30] The reflux was

(1) Nagoya University.
(2) Meijo University.
(3) Nagoya City University.
(4) Ortiz de Montellano, P. R.; Kunze, K. L. *J. Am. Chem. Soc.* **1981**, *103*, 6534.
(5) Saito, S.; Itano, H. A. *Proc. Natl. Acad. Sci. U.S.A.* **1981**, *78*, 5508.
(6) Augusto, O.; Kunze, K. L.; Ortiz de Montellano, P. R. *J. Biol. Chem.* **1982**, *257*, 6231.
(7) Kunze, K. L.; Ortiz de Montellano, P. R. *J. Am. Chem. Soc.* **1983**, *105*, 1380.
(8) Battioni, P.; Mahy, J. P.; Gillet, G.; Mansuy, D. *J. Am. Chem. Soc.* **1983**, *105*, 1399.
(9) Funahashi, S.; Ito, Y.; Kakito, H.; Inamo, M.; Hamada, Y.; Tanaka, M. *Microchim. Acta* **1986**, *I*, 33.
(10) Tabata, M.; Tanaka, M. *Trends Anal. Chem.* **1991**, *10*, 128.
(11) Lavallee, D. K.; Anderson, O. P. *J. Am. Chem. Soc.* **1982**, *104*, 4707.
(12) Goldberg, D. E.; Thomas, K. M. *J. Am. Chem. Soc.* **1976**, *98*, 913.
(13) Anderson, O. P.; Lavallee, D. K. *J. Am. Chem. Soc.* **1976**, *98*, 4670.
(14) Anderson, O. P.; Lavallee, D. K. *J. Am. Chem. Soc.* **1977**, *99*, 1404.
(15) Anderson, O. P.; Lavallee, D. K. *Inorg. Chem.* **1977**, *16*, 1634.
(16) Lavallee, D. K.; Kopelove, A. B.; Anderson, O. P. *J. Am. Chem. Soc.* **1978**, *100*, 3025.
(17) Anderson, O. P.; Kopelove, A. B.; Lavallee, D. K. *Inorg. Chem.* **1980**, *19*, 2101.
(18) Kuila, D.; Lavallee, D. K.; Schauer, C. K.; Anderson, O. P. *J. Am. Chem. Soc.* **1984**, *106*, 448.
(19) Schauer, C. K.; Anderson, O. P.; Lavallee, D. K.; Battioni, J.-P.; Mansuy, D. *J. Am. Chem. Soc.* **1987**, *109*, 3922.
(20) Lavallee, D. K. *The Chemistry and Biochemistry of N-Substituted Porphyrins*; VCH Publishers, Inc.: New York, 1987; pp 7–39.
(21) Balch, A. L.; Cornman, C. R.; Latos-Grażyński, L.; Olmstead, M. M. *J. Am. Chem. Soc.* **1990**, *112*, 7552.
(22) McLaughlin, G. M. *J. Chem. Soc., Perkin Trans. 2* **1974**, 136.
(23) Shah, B.; Shears, B.; Hambright, P. *Inorg. Chem.* **1971**, *10*, 1828.
(24) Bain-Ackerman, M. J.; Lavallee, D. K. *Inorg. Chem.* **1979**, *18*, 3358.
(25) Funahashi, S.; Yamaguchi, Y.; Tanaka, M. *Bull. Chem. Soc. Jpn.* **1984**, *57*, 204.
(26) Lavallee, D. K.; Wite, A.; Diaz, A.; Battioni, J.-P.; Mansuy, D. *Tetrahedron Lett.* **1986**, *27*, 3521.
(27) Bartczak, T. J.; Latos-Grażyński, L.; Wyslouch, A. *Inorg. Chim. Acta* **1990**, *171*, 205.
(28) Funahashi, S.; Yamaguchi, Y.; Tanaka, M. *Inorg. Chem.* **1984**, *23*, 2249.

0020-1669/93/1332-1119$04.00/0

repeated three times with freshly activated molecular sieves. The DMF solution was concentrated under reduced pressure at 50 °C and then cooled. The resultant crystals were filtered under dry nitrogen gas in a drybox. The concentrations of zinc(II) ion in the sample solutions were determined complexometrically using a standard EDTA solution.[31]

Preparation of (5,10,15,20-tetraphenylporphinato)(*o*-tolyl)cobalt(III) ([Co^{III}(TPP)(*o*-Tol)]). Chloro(5,10,15,20-tetraphenylporphinato)cobalt(III) ([CoCl(TPP)]) (100 mg) prepared by a literature method[32] was dissolved in benzene (25 cm^3). To this solution was added *o*-tolyllithium obtained from lithium (100 mg) and *o*-bromotoluene by refluxing in ether. After the solution was allowed to stand for 10 min in the dark, methanol (10 cm^3) was added. The resultant solution was washed with water and dried with sodium sulfate, and then the solvent was removed by evaporation. The residue dissolved in hexane was chromatographed on an alumina column by elution with a cyclohexane/chloroform (7:3 v/v) solution. [Co^{III}(TPP)(*o*-tol)] was obtained from the first red band and recrystallized from a mixture of benzene and methanol. Yield: 91.5%. Secondary ion mass (SI-MS) (*m*/*z*): 762 (M^+). ^{1}H NMR ($CDCl_3$): δ −1.98 (s, 3H, CH_3), −0.45 (d, 1H, *o*-H of *o*-$C_6H_4CH_3$), 4.50 (t, 1H, *m*-H of *o*-$C_6H_4CH_3$), 4.61 (d, 1H, *m*-H of *o*-$C_6H_4CH_3$), 5.23 (t, 1H, *p*-H of *o*-$C_6H_4CH_3$), 7.65 (m, 12H, *m*-H and *p*-H of C_6H_5), 7.93 (m, 8H, *o*-H of C_6H_5), 8.80 (s, 8H, pyrrole H). UV/vis (benzene): λ_{max} (nm) = 411, 530.

Preparation of *N*-*o*-Tolyl-5,10,15,20-tetraphenylporphine (H(*o*-TolTPP)). Trifluoroacetic acid (2 cm^3) was added to a solution containing [Co^{III}(TPP)(*o*-Tol)] (100 mg) in dichloromethane (30 cm^3). The reddish brown solution was stirred at room temperature for 12 h in the dark to obtain a green solution. After the solvent was removed to dryness, the residue was dissolved in dichloromethane and washed with water, diluted ammonia aqueous solution, and three portions of water. The resultant solution was dried with sodium sulfate, and the solvent was again removed. The residue was chromatographed on an alumina column by elution with a chloromethane/benzene (1:9 v/v) solution containing 0.5% triethylamine. The solvent was removed from the green eluate, and the residue was recrystallized from a mixture of benzene and ether. Yield: 65%. Anal. Calcd for $C_{51}H_{36}N_4$: C, 86.96; H, 5.15; N, 7.95. Found: C, 86.81; H, 5.25; N, 7.75. SI-MS (*m*/*z*): 705 (MH^+). ^{1}H NMR ($CDCl_3$): δ 0.10 (d, 1H, *o*-H of *N*-*o*-$C_6H_4CH_3$), 0.95 (broad, NH), 2.10 (s, 3H, CH_3), 3.84 (t, 1H, *m*-H of *N*-*o*-$C_6H_4CH_3$), 5.60 (t, 1H, *p*-H of *N*-*o*-$C_6H_4CH_3$), 5.96 (d, 1H, *m*-H of *N*-*o*-$C_6H_4CH_3$), 6.91 (s, 2H, pyrrole H), 7.7–7.8 (m, 12H, *m*-H and *p*-H of C_6H_5), 8.09 (d, 2H, pyrrole H), 8.17 (d, 4H, *o*-H of C_6H_5), 8.20 (d, 2H, pyrrole H), 8.32 (d, 4H, *o*-H of C_6H_5), 8.62 (s, 2H, pyrrole H). UV/vis ($CHCl_3$ with 1% diethylamine): λ_{max}/nm (log ϵ) = 445 (5.21), 558 sh (3.87), 598 (4.28), 633 sh (3.90), 707 (3.65).

Preparation of *N*-*p*-Tolyl-5,10,15,20-tetraphenylporphine (H(*p*-TolTPP)) and *N*-Phenyl-5,10,15,20-tetraphenylporphine (H(PhTPP)). These N-substituted porphyrins were prepared in benzene using 5,10,15,20-tetraphenylporphinato-*p*-tolylcobalt(III) ([Co(TPP)(*p*-Tol)]) and phenyl-5,10,15,20-tetraphenylporphinatocobalt(III) ([Co(Ph)(TPP)]), respectively, according to a similar method previously reported.[33,34] Yield: 68% for H(*p*-TolTPP) and 87% for H(PhTPP). ^{1}H NMR (CD_3Cl): δ 1.17 (s, 3H, CH_3), 2.81 (d, 2H, *o*-H of *N*-*p*-$C_6H_4CH_3$), 4.97 (d, 2H, *m*-H of *N*-*p*-$C_6H_4CH_3$), 7.19 (s, 2H, pyrrole H), 7.6–7.8 (m, 12H, *m*- and *p*-H of C_6H_5), 8.12 (d, 2H, pyrrole H), 8.14 (d, 4H, *o*-H of C_6H_5), 8.27 (d, 4H, *o*-H of C_6H_5), 8.30 (d, 2H, pyrrole H), 8.62 (s, 2H, pyrrole H) for H(*p*-TolTPP), and 2.95 (d, 2H, *o*-H of *N*-C_6H_5), 5.15 (t, 2H, *m*-H of *N*-C_6H_5), 5.61 (t, 1H, *p*-H of *N*-C_6H_5), 7.21 (s, 2H, pyrrole H), 7.6-7.7 (m, 12H, *m*- and *p*-H of C_6H_5), 8.13 (d, 2H, pyrrole H), 8.14 (d, 4H, *o*-H of C_6H_5), 8.28 (d, 2H, pyrrole H), 8.29 (d, 4H, *o*-H of C_6H_5), 8.62 (s, 2H, pyrrole H) for H(PhTPP). UV/vis ($CHCl_3$ with 1% diethylamine): λ_{max}/nm (log ϵ) = 443 (5.25), 552 sh (3.86), 5.95 (4.26), 633 sh (3.84), 704 (3.68) for H(*p*-TolTPP), and λ_{max}/nm (log ϵ) = 442 (5.24), 552 sh (3.87), 595 (4.25), 633 sh (3.82), 704 (3.67) for H(PhTPP).

Measurements. Kinetic measurements for complexation were performed with a stopped-flow instrument (Type RA 401, Union Giken, Hirakata, Japan). The temperature of the reaction solution was controlled within ±0.1 °C. Rates were measured under pseudo-first-order conditions in DMF solution, i.e., in a large excess of zinc(II) ion concentration over the porphyrin concentration. The H(*o*-TolTPP) concentration was generally (2–8) × 10^{-6} mol kg^{-1}, and the zinc(II) concentration range was 2.8 × 10^{-3} to 1.6 × 10^{-2} mol kg^{-1}. Sodium nitrate (0.9 mol kg^{-1}) was used to maintain the ionic strength. The increase in absorbance at 450 nm was monitored. The pseudo-first-order plot showed good linearity, and the second-order rate constant, *k*, was obtained from the slope. UV–vis spectra were recorded on a Shimadzu UV-240 spectrometer. Mass spectral analysis was carried out on a Hitachi M-80A mass spectrometer. ^{1}H NMR spectra were measured with a JEOL JNM-GX270 FT-NMR spectrometer.

Table I. Summary of Crystal Data and Intensity Collection Parameters for H(*o*-TolTPP)·$^1/_2C_6H_6$·$^1/_2NC_4H_{11}$

formula	$N_{4.5}C_{56}H_{44.5}$	radiation; λ, Å	graphite-monochromated Mo Kα; λ = 0.710 73
*f*w	780.5		
cryst dimens, mm	0.45 × 0.45 × 0.12		
cryst syst	triclinic	2θ range, deg	3–50
space group	$P\bar{1}$	scan technique	ω–2θ
temp, K	295	scan range, deg	1.0 + 0.35 tan θ
a, Å	9.054(1)	scan rate, deg min^{-1}	variable, 1.8–4.1
b, Å	15.369(4)	criterion for obsn	$F_o > 3\sigma(F_o)$
c, Å	16.963(1)	unique obsd data	4954
α, deg	70.30(1)	μ, cm^{-1}	0.66
β, deg	75.64(1)	*R*	0.092
γ, deg	89.42(1)	R_w	0.099
V, Å^3	2145(15)	no. of variables	547
Z	2	GOF	0.99
d_{calcd}, g cm^{-3}	1.208		

Crystal Structure Determination and Refinement. Rhombic crystals suitable for an X-ray analysis were obtained by slow evaporation of a benzene–ether–diethylamine solution of H(*o*-TolTPP). A preliminary examination of a crystal on an Enraf-Nonius CAD4 diffractometer indicated a triclinic unit cell. A least-squares refinement of the setting angles of 25 reflections, collected in the range of 20° < 2θ < 25°, led to the cell constants. Details of the intensity collection parameters and crystal data are summarized in Table I.

The structure was solved by the direct method[35] and refined by the full-matrix least-squares method.[36] Half of a benzene molecule was found as an ordered solvent around a center of symmetry ($^1/_2$, $^1/_2$, 0). Since a disordered diethylamine molecule was located about another center ($^1/_2$, 0, 0) with some complicated orientations, a nitrogen and some carbon atoms were appropriately placed with an occupancy factor of 0.5 or 0.25. All non-hydrogen atoms except those of diethylamine were refined with anisotropic thermal parameters, and the hydrogen atoms bound to carbon were included in the calculated positions. It is suggested from a difference Fourier map that the nitrogen atom of the pyrrole ring opposite to the N-substituted pyrrole ring in H(*o*-TolTPP) is protonated. Final cycles of the two-blocked-matrix least-squares refinement were carried to convergence at $R = 0.092$ and $R_w = 0.099$.[37] Since the final difference Fourier map only showed some 0.30–0.36 e/Å^3 peaks near the peripheral phenyl rings and the dimethylamine, the map was judged to be featureless. The final atomic coordinates are listed in Table II.

Results and Discussion

Characterization. The newly prepared H(*o*-TolTPP) has been characterized by elemental analysis, SI-MS spectrometry, UV–visible spectrophotometry, and ^{1}H NMR spectroscopy. The result of the elemental analysis was in agreement with the proposed formulation. The positive ion SI-MS spectra showed the expected *m*/*z* values for the protonated species, H_2(*o*-TolTPP)$^+$. The absorption spectrum of H(*o*-TolTPP) showed a characteristic spectral pattern similar to those of H(*p*-TolTPP) and H(PhTPP).[18,34]

Signal assignments for the ^{1}H NMR spectrum of H(*o*-TolTPP) have been made by comparison with the spectra of H(*p*-TolTPP)

(29) Arthur, P.; Haynes, W. M.; Varga, L. P. *Anal. Chem.* **1966**, *38*, 1630.
(30) Yano, Y.; Fairhurst, M. T.; Swaddle, T. W. *Inorg. Chem.* **1980**, *19*, 3267.
(31) Schwarzenbach, G.; Flaschka, H. *Complexometric Titration*; Ferdinand Enke, Publisher: Stuttgart, Germany, 1965.
(32) Sakurai, T.; Yamamoto, K.; Naito, H.; Nakamoto, N. *Bull. Chem. Soc. Jpn.* **1976**, *49*, 3042.
(33) Callot, H. J.; Metz, F. *J. Chem. Soc., Chem. Commun.* **1982**, 947.
(34) Callot, H. J.; Metz, F.; Cromer, R. *Nouv. J. Chim.* **1984**, *8*, 759.
(35) Programs of Enraf-Nonius's SDP package were used. The package includes modified versions of Main, Hull, Lessinger, Germain, Declerg, and Woolfson's MULTAN82 and Johnson's ORTEP II.
(36) The program used in the refinement was Scheidt and Haller's (Notre Dame) version of Busing and Levy's ORFLS.
(37) The atomic scattering factors were taken from: *International Tables for X-ray Crystallography*; Kynoch Press: Birmingham, England, 1974; Vol. IV. $R = \sum \|F_o| - |F_c\| / \sum |F_o|$, $R_w = [\sum w(|F_o| - |F_c|)^2 / \sum w(F_o)^2]^{1/2}$ with unit weight.

Table II. Atomic Coordinates for H(*o*-TolTPP)·$^1/_2C_6H_6$·$^1/_2NC_4H_{11}$

atom	x	y	z	B_{eq}, Å^2
N1	0.3160(5)	0.2705(3)	0.4356(3)	2.4(1)
N2	0.2242(5)	0.0859(3)	0.5900(3)	2.7(1)
N3	0.1629(6)	0.1751(3)	0.7181(3)	2.9(1)
N4	0.2258(5)	0.3534(3)	0.5802(3)	2.4(1)
C1	0.2546(6)	0.3546(3)	0.4008(4)	2.6(1)
C2	0.1660(7)	0.3442(4)	0.3490(4)	3.4(2)
C3	0.1662(7)	0.2524(4)	0.3521(4)	3.3(2)
C4	0.2570(6)	0.2072(3)	0.4055(4)	2.6(1)
C5	0.2739(6)	0.1087(3)	0.4360(4)	2.7(1)
C6	0.2727(7)	0.0575(3)	0.5190(4)	2.8(1)
C7	0.3029(7)	−0.0407(4)	0.5501(4)	3.4(2)
C8	0.2686(8)	−0.0696(4)	0.6354(4)	3.8(2)
C9	0.2167(7)	0.0106(4)	0.6606(4)	3.1(1)
C10	0.1608(7)	0.0062(3)	0.7468(4)	3.1(2)
C11	0.1319(7)	0.0831(4)	0.7735(4)	3.1(1)
C12	0.0783(8)	0.0840(4)	0.8588(4)	3.8(2)
C13	0.0829(8)	0.1746(4)	0.8555(4)	3.8(2)
C14	0.1396(7)	0.3219(4)	0.7681(4)	2.9(1)
C15	0.1729(7)	0.3291(4)	0.7342(4)	3.0(2)
C16	0.2258(6)	0.3822(3)	0.6476(4)	2.8(1)
C17	0.2846(7)	0.4796(4)	0.6154(4)	3.1(2)
C18	0.3132(7)	0.5087(4)	0.5298(4)	3.3(2)
C19	0.2751(6)	0.4298(3)	0.5068(4)	2.7(1)
C20	0.2710(6)	0.4350(3)	0.4248(4)	2.7(1)
C21	0.4674(6)	0.2660(3)	0.4491(4)	2.5(1)
C22	0.4887(6)	0.2376(4)	0.5319(4)	2.7(1)
C23	0.6333(7)	0.2348(4)	0.5437(4)	3.4(2)
C24	0.7586(7)	0.2603(4)	0.4742(5)	3.6(2)
C25	0.7364(7)	0.2878(4)	0.3921(4)	3.5(2)
C26	0.5938(7)	0.2921(3)	0.3780(4)	2.9(1)
C27	0.5800(8)	0.3237(4)	0.2848(4)	4.0(2)
C28	0.2678(7)	0.0611(4)	0.3727(4)	3.2(2)
C29	0.3652(9)	0.0920(5)	0.2911(5)	5.1(2)
C30	0.358(1)	0.0464(7)	0.2324(5)	6.8(3)
C31	0.255(1)	−0.0286(6)	0.2581(6)	5.9(3)
C32	0.1570(8)	−0.0588(4)	0.3383(5)	4.4(2)
C33	0.1631(7)	−0.0150(4)	0.3970(4)	3.5(2)
C34	0.1336(8)	−0.0871(4)	0.8167(4)	3.6(2)
C35	0.0247(9)	−0.1512(4)	0.8188(5)	5.7(2)
C36	0.001(1)	−0.2391(5)	0.8839(7)	7.0(3)
C37	0.085(1)	−0.2606(5)	0.9432(6)	6.9(3)
C38	0.195(1)	−0.1987(6)	0.9419(5)	6.5(3)
C39	0.2182(9)	−0.1106(4)	0.8766(5)	5.0(2)
C40	0.1551(7)	0.3768(4)	0.7980(4)	3.0(1)
C41	0.0491(8)	0.4459(4)	0.7955(5)	4.3(2)
C42	0.0425(9)	0.4986(4)	0.8494(5)	4.9(2)
C43	0.135(1)	0.4853(5)	0.9026(5)	5.1(2)
C44	0.2380(9)	0.4189(6)	0.9066(5)	5.4(2)
C45	0.2455(8)	0.3649(4)	0.8537(4)	4.0(2)
C46	0.2630(7)	0.5265(4)	0.3585(4)	3.0(1)
C47	0.1646(7)	0.5894(4)	0.3826(4)	3.6(2)
C48	0.1596(8)	0.6762(4)	0.3222(5)	4.3(2)
C49	0.2462(9)	0.6997(4)	0.2393(5)	5.0(2)
C50	0.3431(9)	0.6382(5)	0.2137(5)	5.0(2)
C51	0.3491(8)	0.5511(4)	0.2742(4)	4.1(2)
C52	0.620(1)	0.454(1)	0.968(1)	9.0(5)
C53	0.527(2)	0.4111(8)	1.0507(8)	8.5(4)
C54	0.596(1)	0.543(1)	0.9170(8)	9.0(5)
C55[a]	0.493(4)	0.028(2)	0.023(2)	11.7(8)[c]
C56[a]	0.501(6)	0.095(3)	−0.034(3)	14(1)[c]
N57[a]	0.361(4)	0.054(3)	−0.002(2)	15.1(9)[c]
C58[a]	0.382(5)	−0.044(3)	0.029(3)	15(1)[c]
C59[b]	0.401(7)	0.155(4)	−0.002(4)	11(1)[c]
C60[b]	0.418(9)	0.116(5)	−0.057(4)	11(2)[c]

[a] Occupancy of 0.5. [b] Occupancy of 0.25. [c] Refined isotropically.

and H(PhTPP) (Figure 1 and Table III). Lavallee et al. assigned the singlets at 7.21 and 8.63 ppm of H(PhTPP) to the β-hydrogens of the N-substituted pyrrole ring (2-H and 3-H) and the pyrrole ring opposite to it (12-H and 13-H) in consideration of the molecular structure.[18] The singlet corresponding to the signal at 7.21 ppm for H(PhTPP) shifts a little upfield (7.19 ppm) in the spectrum for H(*p*-TolTPP) and further upfield (6.91 ppm) for H(*o*-TolTPP), while the singlet at 8.62 ppm does not shift. These facts indicate that the signals in the range 6.91–7.21 ppm are due to 2-H and 3-H, which are sensitive to the difference in the

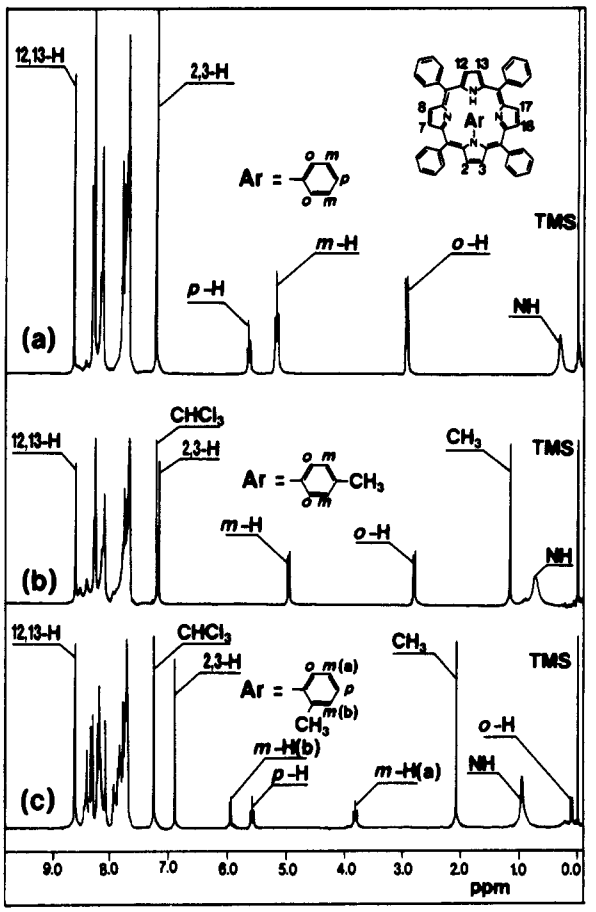

Figure 1. 270-MHz ^{1}H NMR spectra of H(PhTPP) (a), H(*p*-TolTPP) (b), and H(*o*-TolTPP) (c) in $CDCl_3$. Signals in the range 7.6–8.4 ppm are due to 7-H, 8-H, 17-H, and 18-H and peripheral phenyl hydrogens.

Table III. ^{1}H NMR Chemical Shifts of 5,10,15,20-Tetraphenylporphine (TPP) and Some N-Substituted TPP[a] Compounds

	δ (relative to TMS)		
porphyrin	pyrrole	phenyl	N-substituent
TPP[b]	8.75	7.80 (*m*, *p*) 8.30 (*o*)	
MeTPP[c]	7.46 (s), 8.46 (d) 8.64 (d), 8.82 (s)	7.6–7.7 (*m*, *p*) 8.1–8.4 (*o*)	−4.10 (CH_3)
PhTPP	7.21 (s), 8.13 (d) 8.28 (d), 8.63 (s)	7.6–7.7 (*m*, *p*) 8.14, 8.29 (*o*)	2.95 (*o*), 5.15 (*m*) 5.61 (*p*)
p-TolTPP	7.19 (s), 8.12 (d) 8.30 (d), 8.62 (s)	7.6–7.8 (*m*, *p*) 8.14, 8.27 (*o*)	1.17 (CH_3), 2.81 (*o*) 4.97 (*m*)
o-TolTPP	6.91 (s), 8.09 (d) 8.20 (d), 8.62 (s)	7.7–7.8 8.17, 8.32 (*o*)	0.10 (*o*), 2.10 (CH_3) 3.84 (*m*), 5.60 (*p*) 5.96 (*m*)

[a] In $CDCl_3$ unless otherwise cited. [b] In $CDCl_3/CS_2$ solution.[42] [c] In good agreement with the values in ref 43.

N-substituent groups, and that the signals remaining stationary at 8.62 ppm are assignable to 12-H and 13-H.

The *N*-phenyl and *N*-*p*-tolyl groups should rotate at room temperature in $CDCl_3$ because two sets of the ortho and meta hydrogens are equivalent in the NMR time scale in each case. However, in the case of H(*o*-TolTPP), the doublet for *o*-H makes an extraordinary upfield shift, and the triplets for *m*-H(a) and *m*-H(b) are shifted upfield and downfield by ca. 1 ppm, respectively, in comparison with the corresponding hydrogens for H(*p*-TolTPP) (Figure 1). The para hydrogen (*p*-H), however, shows a chemical shift (5.60 ppm) quite similar to that for H(PhTPP) (5.61 ppm). These results clearly show that the *o*-tolyl ring is not rotating under the present conditions. The solid-state structure of H(*o*-TolTPP) (vide infra) also indicates the impossibility of such a rotation. Furthermore, the magnitude of the

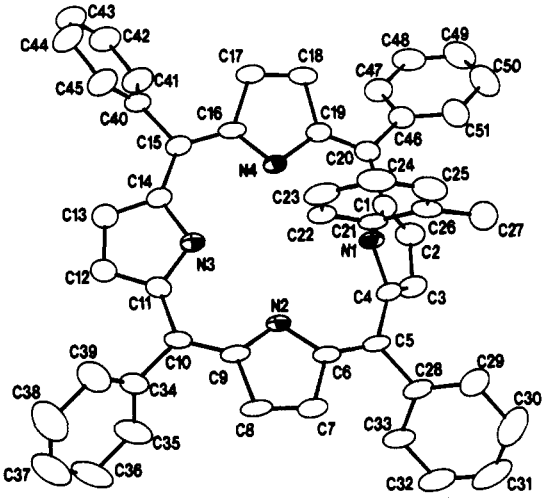

Figure 2. ORTEP diagram of H(*o*-TolTPP) showing the atom-labeling scheme used in all tables. All hydrogen atoms have been omitted.

upfield shifts for the hydrogens on the *o*-tolyl group reveals that the effect of the porphyrin ring current decreases in the following order: *o*-H > *m*-H(a) > *p*-H > *m*-H(b) > methyl protons (almost no ring current effect). This corresponds to the distance from the center of the porphyrin ring.

Another point to be noted is the difference in the ^{1}H NMR chemical shifts of the pyrrolic β-hydrogens depending on both the ring position and the N-substituent groups (Table III). The β-hydrogens of H(*o*-TolTPP) shift upfield in the following order: pyrrole ring opposite to the N-substituted ring (12-H and 13-H) < adjacent pyrrole rings (7-H, 8-H, 17-H, and 18-H) < N-substituted pyrrole ring (2-H and 3-H). This tendency is also observed in the spectra for H(*p*-TolTPP), H(PhTPP), and H(MeTPP). The β-hydrogens of the N-substituted and adjacent rings for H(*o*-TolTPP), H(*p*-TolTPP), and H(PhTPP) shift more upfield than the corresponding hydrogens for H(MeTPP). These results can not be simply explained by the electrochemical properties of the N-substituent groups, because the relatively electron-withdrawing groups, tolyl and phenyl, exhibit the unexpected upfield shift for the β-hydrogens in comparison with the electron-donating methyl group. We may expect the difference in distortion of the porphyrin ring from planarity due to the steric repulsion between the N-substituent groups and porphine ring because the β-hydrogens more removed from the plane of the ring current exhibit a more shielded signal. Therefore, it can be predicted that the N-substituted pyrrole ring is the most highly tilted and the two adjacent rings are secondly tilted in the same porphyrin ring. Furthermore, *N*-*o*-tolyl, *N*-*p*-tolyl, and *N*-phenyl groups may force the N-substituted ring and adjacent rings to be canted more than the *N*-methyl group of H(MeTPP). This prediction can be confirmed by the crystal structure determination.

Crystal Structure of H(*o*-TolTPP). A perspective view of H(*o*-TolTPP) is displayed in Figure 2 along with the atomic numbering scheme. The side-on view emphasizing the distortion of the porphine core is given in Figure 3 with omission of the peripheral phenyl rings for clarity. This structure may be adequate for comparison with the available structure of *N*-methyl-5,10,15,20-tetrakis(*p*-bromophenyl)porphine (H(MeTPPBr$_4$)).[11]

The N-substituted pyrrole ring of H(*o*-TolTPP) (N1-pyrrole ring) forms the most highly canted plane from the N1–N2–N4 reference plane with a dihedral angle of 57.3(2)°. The two adjacent pyrrole rings (N2- and N4-pyrrole rings) are tilted in the direction opposite to that of the N1-pyrrole ring. The dihedral angles are 19.3(2) and 16.4(2)° for the N2- and N4-pyrrole rings, respectively. The protonated N3-pyrrole ring opposite to the N1-pyrrole ring forms an almost coplanar plane with respect to the reference plane (formally the dihedral angle of 1.6(10)° in the same direction as the N1-pyrrole ring). The dihedral angles

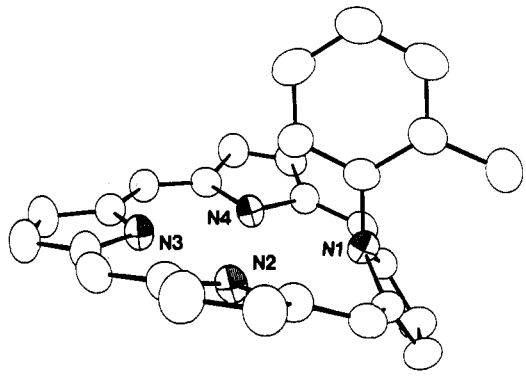

Figure 3. Side-on view of the porphine core of H(*o*-TolTPP) with omission of the peripheral phenyl rings for clarity.

of the N1-pyrrole ring and the N2- and N4-pyrrole rings for H(*o*-TolTPP) are much larger than those of the corresponding rings for H(MeTPPBr$_4$) (27.7° for the N1-pyrrole ring and 10.2 and 11.3° for the N2- and N4-pyrrole rings, respectively), though the N3-pyrrole ring for H(*o*-TolTPP) is less canted than that for H(MeTPPBr$_4$) (8.1°) in the same direction as the N1-pyrrole ring.[11] Consequently, the bulkier *N*-*o*-tolyl group compels the porphine ring system to be more distorted than the *N*-methyl group.

In spite of a lack of structure determination of free base N-substituted porphyrins, extensive studies for the structures of N-substituted metalloporphyrins have been performed.[12-21] Lavallee et al. have determined the crystal structures of chlorozinc(II) complexes of N-substituted porphyrins such as [Zn(PhTPP)Cl],[18,19] [Zn(MeTPP)Cl],[16,19] and [Zn(BzTPP)Cl],[19] which will give information about metal ion incorporation. In the solid state structures of the metalloporphyrins, the three non-N-substituted pyrrole rings are tilted in the direction opposite to that of the N-substituted pyrrole ring to bind a metal ion with similar bond distances. The slants of the three non-N-substituted pyrrole rings are correlated with the slant of the N-substituted pyrrole ring in the opposite direction. A similar tendency in distortion is observed in the free base porphyrins though the N3-pyrrole ring can be hardly tilted in the direction opposite to the N1-pyrrole ring without a metal ion being bound. In comparison between the dihedral angles of N3-pyrrole rings for H(*o*-tolTPP) (coplanar) and H(MeTPPBr$_4$) (8.1° in the same direction as the N1-pyrrole ring), the distorted structure of the former is more similar to those for the metalloporphyrins than that of the latter is. Furthermore, the larger dihedral angles of N2- and N4-pyrrole rings for H(TolTPP) can be a greater advantage for metal ion incorporation than those for H(MeTPPBr$_4$). The difference in reactivity for metalation between *N*-methyl and *N*-*o*-tolyl porphyrins has been established as described below.

We can expect a correlation between the ^{1}H NMR chemical shift for the β-hydrogens on the pyrrole rings and the tilt of the pyrrole rings from the reference porphyrin plane, as noted above; the increase of the dihedral angles of the pyrrole rings promotes the upfield shift of β-hydrogens because of removal from the plane of the ring current. In fact, the order of the upfield shifts: N3-pyrrole ring < N2- and N4-pyrrole rings < N1-pyrrole ring, corresponds to the increase in the dihedral angle. In addition, the further upfield shifts for the N1-, N2-, and N4-pyrrole rings for H(*o*-TolTPP) are clearly shown in comparison with the corresponding ring for H(MeTPP) which may be less canted as in the case of H(MeTPPBr$_4$). From the chemical shifts for the β-hydrogens (see Table III), the dihedral angles of the N-substituted and adjacent rings for H(*p*-TolTPP) and H(PhTPP) can be expected to be larger than those for H(MeTPP), respectively.

It should be pointed out here that the angle between the N1–C21 bond and the plane of the C1–N1–C4 triangle (Figure 2) is ca. 152°, which is deviated from 180° due to the steric repulsion between the *N*-*o*-tolyl group and the porphine ring. This indicates

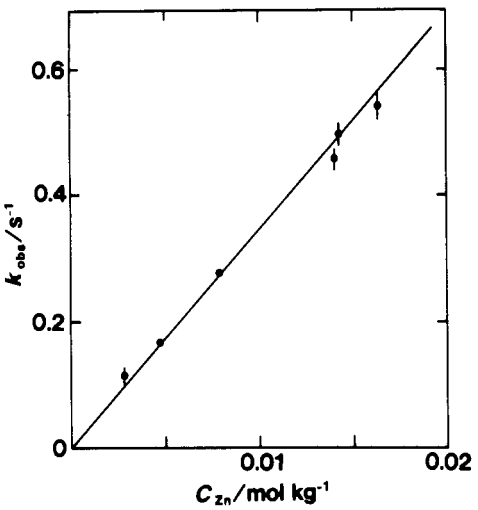

Figure 4. Dependence of conditional first-order rate constant, $k_{0(Zn)}$, on the Zn(II) ion concentration. Vertical bar shows the error range of each point, which corresponds to the average value of eight determinations.

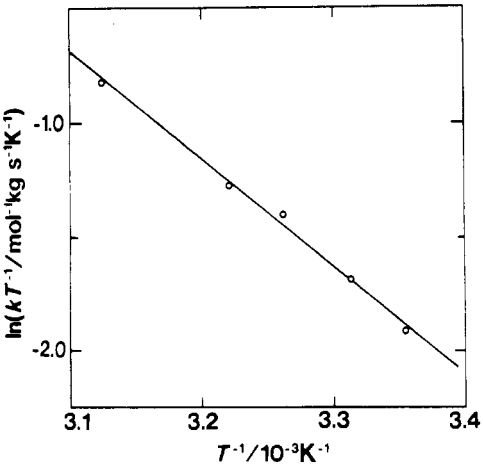

Figure 5. Temperature dependence of the second-order rate constant.

Table IV. Rate Constants and Activation Parameters for Complexation of H(o-TolTPP) and H(MeTPP) with Zn(II) Ion in DMF

porphyrin	k(25 °C), mol^{-1} kg s^{-1}	$\Delta H^{\ddagger}$, kJ mol^{-1}	$\Delta S^{\ddagger}$, J K^{-1} mol^{-1}
H(o-TolTPP)	35 ± 1	39 ± 2	−88 ± 6
H(MeTPP)[a]	10.4 ± 0.8	59 ± 3	−28 ± 11

[a] Reference 28.

that the N1 nitrogen with three bond angles, 121.6(4), 122.6(4), and 106.0(5)°, has a sp^2–sp^3 mixed character. Thus, the conjugated system including the π-electrons of the o-tolyl group and the N1-pyrrole ring is partially broken due to the deviation from planarity (sp^2 character) of the pyrrole nitrogen. This steric restriction reduces the substituent effect of the N-tolyl and N-phenyl groups on the β-hydrogens of the N1-pyrrole ring which might suffer the downfield shift due to the electron-withdrawing property of the π-delocalization system.

Kinetics. Conditional first-order rate constants, $k_{0(Zn)}$, for the incorporation reaction 1 of Zn(II) ion into H(o-TolTPP) in DMF solution are proportional to Zn(II) ion concentrations (C_{Zn}) as shown in Figure 4. Thus, the complex formation reaction is first

$$H(o\text{-TolTPP}) + Zn^{2+} \rightarrow [Zn(o\text{-TolTPP})]^{+} + H^{+} \quad (1)$$

order with respect to the porphyrin and Zn(II) ion concentrations: $k_{0(Zn)} = k[Zn^{2+}]$. The visible spectrum after completion of the reaction has the absorption maxima at 450, 573, 632, and 675 nm. This spectral pattern is similar to those of Zn(II) complexes with analogous N-substituted porphyrins such as [Zn(PhTPP)Cl] and [Zn(MeTPP)Cl].[18] The second-order rate constants, k, were obtained at various temperatures. The temperature dependence of k is given in Figure 5 according to the Eyring plot. The values of k at 25 °C, activation enthalpy ($\Delta H^{\ddagger}$), and activation entropy ($\Delta S^{\ddagger}$) are summarized in Table IV together with those for the complexation of H(MeTPP).

The complexation rate for H(o-TolTPP) is appreciably faster than that for H(MeTPP).[23-25,28] For metalloporphyrin formation of H(MeTPP), it has been proposed that the rapid deformation equilibrium of the porphine core precedes the rate-determining solvent loss.[28] Applying this reaction process to the complexation of H(o-TolTPP), it is suggested that the difference in rate between the metalloporphyrin formations for H(o-TolTPP) and H(MeTPP) reflects the difference in the deformation. The crystal structures show a more favorable distortion of H(o-TolTPP) for the complexation rather than $H(MeTPPBr_4)$ which has basically the same N-methylporphine core as H(MeTPP). It should be again emphasized that the bulkiness of the N-substituent group enhances the reactivity.

The metalloporphyrin formation of H(o-TolTPP) with Zn(II) ion in DMF can be expected to proceed through essentially the same reaction mechanism as that of H(MeTPP) which proceeds via the dissociative interchange mechanism.[28] The value of $\Delta H^{\ddagger}$ for the formation of $[Zn(o\text{-TolTPP})]^{+}$ is lower than that of $[Zn(MeTPP)]^{+}$, and the value of $\Delta S^{\ddagger}$ for the former is more negative than that for the latter. These different values may reveal that the metalloporphyrin formation for H(o-TolTPP) may be activated by a less dissociative mode than that for H(MeTPP).[38] Considering that the N2- and N4-pyrrole rings for the H(o-TolTPP) ligand are more highly canted in the direction opposite to the N1-pyrrole ring than those for H(MeTPP), the N2- and N4-nitrogen donor atoms of H(o-TolTPP) can be more easily inserted into the first coordination sphere of the solvated Zn(II) ion than those for H(MeTPP). The difference in structure between the H(o-TolTPP) and H(MeTPP) cores suggests that the bond formation can be more highly promoted in the transition state for the formation of $[Zn(o\text{-TolTPP})]^{+}$ than that of $[Zn(MeTPP)]^{+}$.

Lavallee et al. have reported the synthesis of the water-soluble porphyrins with carboxyl and sulfonic acid groups,[39] and we have succeeded in isolating the possible isomers of sulfonated PhTPP.[40,41] From an analytical point of view, water-soluble porphyrins are very useful as reagents for trace-metal analysis.[9,10] However, a disadvantage is the fact that the metalation rate of porphyrin is not fast enough. From the present results, it is expected that we can overcome such a problem by taking advantage of the steric effect of an N-substituted group.

Acknowledgment. This work was supported by Grants-in-Aid for Scientific Research on Priority Area No. 04215105 and for Scientific Research No. 04403011 from the Ministry of Education, Science, and Culture of Japan.

Supplementary Material Available: Tables A–D, listing anisotropic thermal parameters, bond distances, bond angles for non-hydrogen atoms, and hydrogen positional parameters of $H(o\text{-TolTPP})\cdot{}^{1}/_{2}C_6H_6\cdot{}^{1}/_{2}C_4H_{11}N$ (7 pages). Ordering information is given on any current masthead page.

(38) Tanaka, M. *Inorg. Chim. Acta* **1981**, *54*, L129.
(39) Mercer-Smith, J. A.; Roberts, J. C.; Figard, S. D.; Lavallee, D. K. In *Targeted Diagnosis and Therapy Series*; Rodwell, J. T., Ed.; Marcel Dekker: New York, 1988; Vol. 1, pp 317–352.
(40) Shimizu, Y.; Taniguchi, K.; Inada, Y.; Funahashi, S.; Tsuda, Y.; Ito, Y.; Inamo, M.; Tanaka, M. *Bull. Chem. Soc. Jpn.* **1992**, *65*, 771.
(41) Tsuda, Y.; Ito, Y. Manuscript in preparation.
(42) Storm, C. B.; Teklu, Y.; Sokolshi, E. A. *Ann. N.Y. Acad. Sci.* **1973**, *206*, 631.
(43) Al-Hazimi, H. M. G.; Jackson, A. H.; Johnson, A. W.; Winter, M. *J. Chem. Soc. Perkin Trans. I* **1977**, 98.